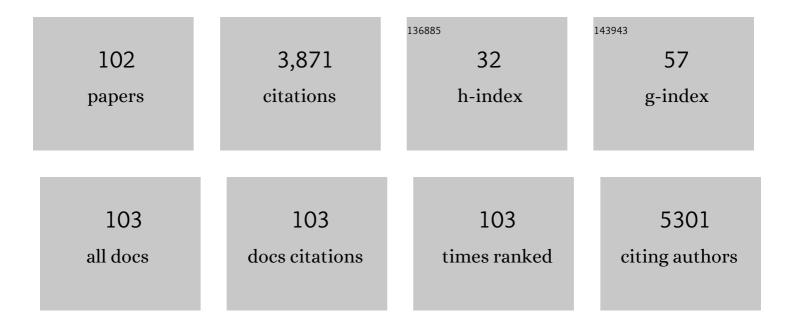
List of Publications by Year in descending order

Source: https://exaly.com/author-pdf/7965926/publications.pdf Version: 2024-02-01



#	Article	IF	CITATIONS
1	Recognizing the Mechanism of Sulfurized Polyacrylonitrile Cathode Materials for Li–S Batteries and beyond in Al–S Batteries. ACS Energy Letters, 2018, 3, 2899-2907.	8.8	224
2	The structure and binding mode of citrate in the stabilization of gold nanoparticles. Nature Chemistry, 2017, 9, 890-895.	6.6	222
3	Structure–performance descriptors and the role of Lewis acidity in the methanol-to-propylene process. Nature Chemistry, 2018, 10, 804-812.	6.6	221
4	Sn surface-enriched Pt–Sn bimetallic nanoparticles as a selective and stable catalyst for propane dehydrogenation. Journal of Catalysis, 2014, 320, 52-62.	3.1	144
5	Effect of Zeolite Topology and Reactor Configuration on the Direct Conversion of CO ₂ to Light Olefins and Aromatics. ACS Catalysis, 2019, 9, 6320-6334.	5.5	144
6	Synthesis of single-crystal-like nanoporous carbon membranes and their application in overall water splitting. Nature Communications, 2017, 8, 13592.	5.8	142
7	Cooperative Effect of Monopodal Silica-Supported Niobium Complex Pairs Enhancing Catalytic Cyclic Carbonate Production. Journal of the American Chemical Society, 2015, 137, 7728-7739.	6.6	123
8	Highly Stable Phosphonateâ€Based MOFs with Engineered Bandgaps for Efficient Photocatalytic Hydrogen Production. Advanced Materials, 2020, 32, e1906368.	11.1	117
9	WMe6 Tamed by Silica: ≡Si–O–WMe5 as an Efficient, Well-Defined Species for Alkane Metathesis, Leading to the Observation of a Supported W–Methyl/Methylidyne Species. Journal of the American Chemical Society, 2014, 136, 1054-1061.	6.6	84
10	A Supramolecular View on the Cooperative Role of BrÃ,nsted and Lewis Acid Sites in Zeolites for Methanol Conversion. Journal of the American Chemical Society, 2019, 141, 14823-14842.	6.6	80
11	[Cu ₆₁ (S ^t Bu) ₂₆ S ₆ Cl ₆ H ₁₄] ^{+< A Core–Shell Superatom Nanocluster with a Quasi-<i>J</i> an "18-Crown-6―Metal-Sulfide-like Stabilizing Belt. , 2019, 1, 297-302.}	:/sup>:	76
12	Single-Site VO _{<i>x</i>} Moieties Generated on Silica by Surface Organometallic Chemistry: A Way To Enhance the Catalytic Activity in the Oxidative Dehydrogenation of Propane. ACS Catalysis, 2016, 6, 5908-5921.	5.5	74
13	Smart covalent organic networks (CONs) with "on-off-on―light-switchable pores for molecular separation. Science Advances, 2020, 6, eabb3188.	4.7	71
14	Alkane Metathesis with the Tantalum Methylidene [(≡SiO)Ta(╀H ₂)Me ₂]/[(≡SiO) ₂ Ta(╀H ₂)Me] Genera from Well-Defined Surface Organometallic Complex [(≡SiO)Ta ^V Me ₄]. Journal of the American Chemical Society, 2015, 137, 588-591.	ted 6.6	65
15	On the dynamic nature of Mo sites for methane dehydroaromatization. Chemical Science, 2018, 9, 4801-4807.	3.7	65
16	One-step electrochemical modification of carbon nanotubes by ruthenium complexes via new diazonium salts. Journal of Electroanalytical Chemistry, 2008, 621, 277-285.	1.9	64
17	Conversion of actual flue gas CO 2 via cycloaddition to propylene oxide catalyzed by a single-site, recyclable zirconium catalyst. Journal of CO2 Utilization, 2017, 20, 243-252.	3.3	60
18	Tandem Conversion of CO ₂ to Valuable Hydrocarbons in Highly Concentrated Potassium Iron Catalysts. ChemCatChem, 2019, 11, 2879-2886.	1.8	57

#	Article	IF	CITATIONS
19	Reactive surface organometallic complexes observed using dynamic nuclear polarization surface enhanced NMR spectroscopy. Chemical Science, 2017, 8, 284-290.	3.7	55
20	Heterostructured MXene and g-C3N4 for high-rate lithium intercalation. Nano Energy, 2019, 65, 104030.	8.2	54
21	Controlling the hydrogenolysis of silica-supported tungsten pentamethyl leads to a class of highly electron deficient partially alkylated metal hydrides. Chemical Science, 2016, 7, 1558-1568.	3.7	53
22	Acidity modification of ZSM-5 for enhanced production of light olefins from CO2. Journal of Catalysis, 2020, 381, 347-354.	3.1	52
23	[(2SiO)Ta ^V Cl ₂ Me ₂]: A Wellâ€Defined Silicaâ€Supported Tantalum(V) Surface Complex as Catalyst Precursor for the Selective Cocatalystâ€Free Trimerization of Ethylene. Angewandte Chemie - International Edition, 2012, 51, 11886-11889.	7.2	45
24	Carbon nanotubes and helical carbon nanofibers grown by chemical vapour deposition on C60 fullerene supported Pd nanoparticles. Carbon, 2011, 49, 1101-1107.	5.4	44
25	Polytriazole membranes with ultrathin tunable selective layer for crude oil fractionation. Science, 2022, 376, 1105-1110.	6.0	44
26	Extremely Hydrophobic POPs to Access Highly Porous Storage Media and Capturing Agent for Organic Vapors. CheM, 2019, 5, 180-191.	5.8	42
27	Polymerization of conducting polymers inside carbon nanotubes. Chemical Physics Letters, 2006, 431, 139-144.	1.2	41
28	Use of the Phenâ€NaDPO:Sn(SCN) ₂ Blend as Electron Transport Layer Results to Consistent Efficiency Improvements in Organic and Hybrid Perovskite Solar Cells. Advanced Functional Materials, 2019, 29, 1905810.	7.8	41
29	A site-sensitive quasi-in situ strategy to characterize Mo/HZSM-5 during activation. Journal of Catalysis, 2019, 370, 321-331.	3.1	40
30	High-Purity Diamagnetic Single-Wall Carbon Nanotube Buckypaper. Chemistry of Materials, 2007, 19, 2982-2986.	3.2	39
31	A Silica-Supported Monoalkylated Tungsten Dioxo Complex Catalyst for Olefin Metathesis. ACS Catalysis, 2018, 8, 2715-2729.	5.5	38
32	Initial Carbonâ^'Carbon Bond Formation during the Early Stages of Methane Dehydroaromatization. Angewandte Chemie - International Edition, 2020, 59, 16741-16746.	7.2	36
33	Well-Defined Surface Species [(≡Si—O—)W(â•O)Me ₃] Prepared by Direct Methylation of [(≡Si—O—)W(â•O)Cl ₃], a Catalyst for Cycloalkane Metathesis and Transformation of Ethylene to Propylene. ACS Catalysis, 2015, 5, 2164-2171.	5.5	35
34	Synergy between Two Metal Catalysts: A Highly Active Silica-Supported Bimetallic W/Zr Catalyst for Metathesis of <i>n</i> -Decane. Journal of the American Chemical Society, 2016, 138, 8595-8602.	6.6	34
35	Bimetallic Pt-Sn nanocluster from the hydrogenolysis of a well-defined surface compound consisting of [(AIO)Pt(COD)Me] and [(AIO)SnPh3] fragments for propane dehydrogenation. Journal of Catalysis, 2019, 374, 391-400.	3.1	34
36	Coated sulfated zirconia/SAPO-34 for the direct conversion of CO ₂ to light olefins. Catalysis Science and Technology, 2020, 10, 1507-1517.	2.1	34

#	Article	IF	CITATIONS
37	Bipodal Surface Organometallic Complexes with Surface N-Donor Ligands and Application to the Catalytic Cleavage of C–H and C–C Bonds in n-Butane. Journal of the American Chemical Society, 2013, 135, 17943-17951.	6.6	33
38	TiO ₂ -supported Pt single atoms by surface organometallic chemistry for photocatalytic hydrogen evolution. Physical Chemistry Chemical Physics, 2019, 21, 24429-24440.	1.3	32
39	Unearthing a Well-Defined Highly Active Bimetallic W/Ti Precatalyst Anchored on a Single Silica Surface for Metathesis of Propane. Journal of the American Chemical Society, 2017, 139, 3522-3527.	6.6	30
40	Surface enhanced dynamic nuclear polarization solid-state NMR spectroscopy sheds light on BrÃ,nsted–Lewis acid synergy during the zeolite catalyzed methanol-to-hydrocarbon process. Chemical Science, 2019, 10, 8946-8954.	3.7	30
41	Routes to the synthesis of carbon nanotube–polyacetylene composites by Ziegler–Natta polymerization of acetylene inside carbon nanotubes. Current Applied Physics, 2007, 7, 39-41.	1.1	29
42	Hydrogenation of C ₆₀ in Peapods: Physical Chemistry in Nano Vessels. Journal of Physical Chemistry C, 2009, 113, 8583-8587.	1.5	29
43	Quantifying the impact of dispersion, acidity and porosity of Mo/HZSM-5 on the performance in methane dehydroaromatization. Applied Catalysis A: General, 2019, 574, 144-150.	2.2	28
44	Effect of Support on Metathesis of <i>n</i> â€Decane: Drastic Improvement in Alkane Metathesis with WMe ₅ Linked to Silica–Alumina. Chemistry - A European Journal, 2015, 21, 6100-6106.	1.7	27
45	Impact of small promoter amounts on coke structure in dry reforming of methane over Ni/ZrO ₂ . Catalysis Science and Technology, 2020, 10, 3965-3974.	2.1	27
46	Spray-coated graphene oxide hollow fibers for nanofiltration. Journal of Membrane Science, 2020, 606, 118006.	4.1	27
47	Isolation and Characterization of Wellâ€Defined Silicaâ€Supported Azametallacyclopentane: A Key Intermediate in Catalytic Hydroaminoalkylation Reactions. Advanced Synthesis and Catalysis, 2015, 357, 3148-3154.	2.1	26
48	Well-defined silica-supported zirconium–imido complexes mediated heterogeneous imine metathesis. Chemical Communications, 2016, 52, 4617-4620.	2.2	26
49	A well-defined mesoporous amine silica surface via a selective treatment of SBA-15 with ammonia. Chemical Communications, 2012, 48, 3067.	2.2	25
50	Direct Functionalization of Nanodiamonds with Maleimide. Chemistry of Materials, 2014, 26, 2766-2769.	3.2	25
51	Morphology control of anatase TiO2 for well-defined surface chemistry. Physical Chemistry Chemical Physics, 2018, 20, 14362-14373.	1.3	25
52	Confined adamantane molecules assembled to one dimension in carbon nanotubes. Carbon, 2011, 49, 1159-1166.	5.4	24
53	Methane Reacts with Heteropolyacids Chemisorbed on Silica to Produce Acetic Acid under Soft Conditions. Journal of the American Chemical Society, 2013, 135, 804-810.	6.6	24
54	Predicting the DNP-SENS efficiency in reactive heterogeneous catalysts from hydrophilicity. Chemical Science, 2018, 9, 4866-4872.	3.7	24

#	Article	IF	CITATIONS
55	SOMC-Designed Silica Supported Tungsten Oxo Imidazolin-2-iminato Methyl Precatalyst for Olefin Metathesis Reactions. Inorganic Chemistry, 2017, 56, 861-871.	1.9	23
56	A Silica-Supported Double-Decker Silsesquioxane Provides a Second Skin for the Selective Generation of Bipodal Surface Organometallic Complexes. Organometallics, 2012, 31, 7610-7617.	1.1	22
57	Low temperature activation of methane over a zinc-exchanged heteropolyacid as an entry to its selective oxidation to methanol and acetic acid. Chemical Communications, 2014, 50, 12348-12351.	2.2	22
58	Facile and Efficient Synthesis of the Surface Tantalum Hydride (≡SiO) ₂ Ta ^{III} H and Tris-Siloxy Tantalum (≡SiO) ₃ Ta ^{III} Starting from Novel Tantalum Surface Species (≡SiO)TaMe ₄ and (≡SiO) ₂ TaMe ₃ . Organometallics, 2014 1205-1211.	, 33 <mark>.1</mark>	22
59	Well-defined silica supported aluminum hydride: another step towards the utopian single site dream?. Chemical Science, 2015, 6, 5456-5465.	3.7	22
60	Aromatization of Ethylene – Main Intermediate for MDA?. ChemCatChem, 2020, 12, 544-549.	1.8	22
61	Organosilane with Gemini-Type Structure as the Mesoporogen for the Synthesis of the Hierarchical Porous ZSM-5 Zeolite. Langmuir, 2016, 32, 2085-2092.	1.6	21
62	Organic solvent and thermal resistant polytriazole membranes with enhanced mechanical properties cast from solutions in non-toxic solvents. Journal of Membrane Science, 2020, 597, 117634.	4.1	21
63	Well-defined azazirconacyclopropane complexes supported on silica structurally determined by 2D NMR comparative elucidation. Chemical Communications, 2013, 49, 4616.	2.2	20
64	lmine Metathesis Catalyzed by a Silica-Supported Hafnium Imido Complex. ACS Catalysis, 2018, 8, 9440-9446.	5.5	20
65	Benzimidazole linked polymers (BILPs) in mixed-matrix membranes: Influence of filler porosity on the CO2/N2 separation performance. Journal of Membrane Science, 2018, 566, 213-222.	4.1	20
66	Room-Temperature Reactivity Of Silicon Nanocrystals With Solvents: The Case Of Ketone And Hydrogen Production From Secondary Alcohols: Catalysis?. ACS Applied Materials & Interfaces, 2015, 7, 13794-13800.	4.0	19
67	Solidâ€State NMR and DFT Studies on the Formation of Wellâ€Defined Silicaâ€Supported Tantallaaziridines: From Synthesis to Catalytic Application. Chemistry - A European Journal, 2016, 22, 3000-3008.	1.7	18
68	Exploiting the interactions between the ruthenium Hoveyda–Grubbs catalyst and Al-modified mesoporous silica: the case of SBA15 <i>vs.</i> KCC-1. Chemical Science, 2018, 9, 3531-3537.	3.7	18
69	Single-Site Tetracoordinated Aluminum Hydride Supported on Mesoporous Silica. From Dream to Reality!. Organometallics, 2016, 35, 3288-3294.	1.1	17
70	Atomic-level organization of vicinal acid–base pairs through the chemisorption of aniline and derivatives onto mesoporous SBA15. Chemical Science, 2016, 7, 6099-6105.	3.7	16
71	Hybrid electrolytes based on ionic liquids and amorphous porous silicon nanoparticles: Organization and electrochemical properties. Applied Materials Today, 2017, 9, 10-20.	2.3	16
72	Docking of tetra-methyl zirconium to the surface of silica: a well-defined pre-catalyst for conversion of CO ₂ to cyclic carbonates. Chemical Communications, 2020, 56, 3528-3531.	2.2	16

#	Article	IF	CITATIONS
73	Wellâ€Defined Singleâ€Site Monohydride Silicaâ€Supported Zirconium from Azazirconacyclopropane. Chemistry - A European Journal, 2015, 21, 4294-4299.	1.7	15
74	Mechanistic Study of Hydroamination of Alkyne through Tantalum-Based Silica-Supported Surface Species. ACS Catalysis, 2019, 9, 8719-8725.	5.5	15
75	From single-site tantalum complexes to nanoparticles of Ta _x N _y and TaO _x N _y supported on silica: elucidation of synthesis chemistry by dynamic nuclear polarization surface enhanced NMR spectroscopy and X-ray absorption spectroscopy. Chemical Science, 2017, 8, 5650-5661.	3.7	14
76	Clean chlorination of silica surfaces by a single-site substitution approach. Dalton Transactions, 2018, 47, 4301-4306.	1.6	14
77	Tungsten(VI) Carbyne/Bis(carbene) Tautomerization Enabled by Nâ€Donor SBA15 Surface Ligands: A Solidâ€State NMR and DFT Study. Angewandte Chemie - International Edition, 2016, 55, 11162-11166.	7.2	13
78	Tetracrystalline Tetrablock Quarterpolymers: Four Different Crystallites under the Same Roof. Angewandte Chemie - International Edition, 2019, 58, 16267-16274.	7.2	13
79	Well-defined mono(η3-allyl)nickel complex î€,MONi(η3-C3H5) (M = Si or Al) grafted onto silica or alumina: a molecularly dispersed nickel precursor for syntheses of supported small size nickel nanoparticles. Chemical Communications, 2014, 50, 7716.	2.2	12
80	Well-Defined Silica Grafted Molybdenum Bis(imido) Catalysts for Imine Metathesis Reactions. Organometallics, 2017, 36, 1550-1556.	1.1	12
81	Non-oxidative dehydrogenation of isobutane over supported vanadium oxide: nature of the active sites and coke formation. Catalysis Science and Technology, 2020, 10, 6139-6151.	2.1	12
82	Rapid fabrication of MOF-based mixed matrix membranes through digital light processing. Materials Advances, 2021, 2, 2739-2749.	2.6	12
83	SOMC grafting of vanadium oxytriisopropoxide (VO(O ⁱ Pr) ₃) on dehydroxylated silica; analysis of surface complexes and thermal restructuring mechanism. RSC Advances, 2018, 8, 20801-20808.	1.7	11
84	Synthesis and characterization of a homogeneous and silica supported homoleptic cationic tungsten(<scp>vi</scp>) methyl complex: application in olefin metathesis. Chemical Communications, 2016, 52, 11270-11273.	2.2	10
85	CO ₂ activation through silylimido and silylamido zirconium hydrides supported on N-donor chelating SBA15 surface ligands. Chemical Communications, 2016, 52, 2577-2580.	2.2	10
86	[(SiO)TaV(CH2)Cl2], the first tantalum methylidene species prepared and identified on the silica surface. Journal of Organometallic Chemistry, 2013, 744, 3-6.	0.8	9
87	Single site silica supported tetramethyl niobium by the SOMC strategy: synthesis, characterization and structure–activity relationship in the ethylene oligomerization reaction. Chemical Communications, 2017, 53, 7068-7071.	2.2	9
88	Solventâ€Free Synthesis of Quaternary Metal Sulfide Nanoparticles Derived from Thiourea. Particle and Particle Systems Characterization, 2018, 35, 1700183.	1.2	7
89	A strategy to convert propane to aromatics (BTX) using TiNp ₄ grafted at the periphery of ZSM-5 by surface organometallic chemistry. Dalton Transactions, 2019, 48, 6611-6620.	1.6	6
90	The Importance of Thermal Treatment on Wet-Kneaded Silica–Magnesia Catalyst and Lebedev Ethanol-to-Butadiene Process. Nanomaterials, 2021, 11, 579.	1.9	5

#	Article	IF	CITATIONS
91	Investigation of Surface Alkylation Strategy in SOMC: In Situ Generation of a Silica-Supported Tungsten Methyl Catalyst for Cyclooctane Metathesis. Organometallics, 2016, 35, 2524-2531.	1.1	4
92	Chemical and Structural Analysis of Carbon Materials Subjected to Alkaline Oxidation. ACS Omega, 2019, 4, 18725-18733.	1.6	4
93	Titanium methyl tamed on silica: synthesis of a well-defined pre-catalyst for hydrogenolysis of <i>n</i> -alkane. Chemical Communications, 2020, 56, 13401-13404.	2.2	4
94	Electromagnetic Properties of Inner Double Walled Carbon Nanotubes Investigated by Nuclear Magnetic Resonance. Journal of Nanomaterials, 2013, 2013, 1-6.	1.5	3
95	Initial Carbonâ^'Carbon Bond Formation during the Early Stages of Methane Dehydroaromatization. Angewandte Chemie, 2020, 132, 16884.	1.6	3
96	The use of a well-defined surface organometallic complex as a probe molecule: [(ĩ€,SiO)Ta ^V Cl ₂ Me ₂] shows different isolated silanol sites on the silica surface. Chemical Communications, 2014, 50, 11721-11723.	2.2	2
97	Cationic Tungsten(VI) Penta-Methyl Complex: Synthesis, Characterization and its Application in Olefin Metathesis Reaction. Oil and Gas Science and Technology, 2016, 71, 21.	1.4	2
98	Tungsten Catalyst Incorporating a Wellâ€Defined Tetracoordinated Aluminum Surface Ligand for Selective Metathesis of Propane, [(≡Siâ~'Oâ~'Si≡)(≡Siâ^'Oâ~') ₂ Alâ^'Oâ^'W(≡C <i>t</i> Bu) (H) ₂]. ChemCatChem, 2019, 11, 614-620.	1.8	2
99	Rigid, non-porous and tunable hybrid p-aminobenzoate/TiO2 materials: Toward a fine structural determination of the immobilized RhCl(Ph3)3 complex. Journal of Organometallic Chemistry, 2015, 784, 103-108.	0.8	1
100	Synthesis and Characterization of Cationic Tetramethyl Tantalum(V) Complex. Catalysts, 2018, 8, 507.	1.6	1
101	Tetracrystalline Tetrablock Quarterpolymers: Four Different Crystallites under the Same Roof. Angewandte Chemie, 2019, 131, 16413-16420.	1.6	1
102	The elemental analysis and multi-nuclear NMR study of an alkali molten salt used to digest reference and commercial SWCNT powders. Journal of Analytical Atomic Spectrometry, 2020, 35, 2758-2769.	1.6	1